

Can Decentralized Control Outperform Centralized? The Role of Communication Latency

Luca Ballotta^{1b}, *Graduate Student Member, IEEE*,
Mihailo R. Jovanović^{1b}, *Fellow, IEEE*, and Luca Schenato^{1b}, *Fellow, IEEE*

Abstract— In this paper, we examine the influence of communication latency on performance of networked control systems. Even though distributed control architectures offer advantages in terms of communication, maintenance costs, and scalability, it is an open question how communication latency that varies with network topology influences closed-loop performance. For networks in which delays increase with the number of links, we establish the existence of a fundamental performance trade-off that arises from control architecture. In particular, we utilize consensus dynamics with single- and double-integrator agents to show that, if delays increase fast enough, a sparse controller with nearest neighbor interactions can outperform the centralized one with all-to-all communication topology.

Index Terms—Communication latency, control architecture, distributed control, network optimization.

I. INTRODUCTION

IT IS widely accepted that modern multi-agent systems cannot rely on centralized control architectures. This conclusion stems from issues related to gathering all decision making to a central node, ranging from lack of robustness and failures proneness, to maintenance costs, and communication overhead. Indeed, large-scale networks have experienced a net shift towards decentralized and distributed architectures [1], [2]. Moreover, the recent deployment of powerful communication protocols for massive networks, *e.g.*, 5G [3], [4], and advances in embedded electronics [5], [6], as well as in algorithms for low-power devices (*e.g.*, TinyML [7]), which allow to spread computational tasks across network nodes according to edge- and fog-computing paradigms [8]–[10], are making such networked systems grow at unprecedented scale, further stressing the importance of distributed controller architectures.

A challenging issue in large-scale wireless network systems is the latency arising from channel constraints, such as limited bandwidth or packet retransmissions. To address this problem, research efforts have been moving towards two main directions.

Related work in control theory deals with control design for distributed architectures, where classical methods, such

as LQG or $\mathcal{H}_2/\mathcal{H}_\infty$ control, [require an all-to-all information exchange which is infeasible for large-scale systems](#).

A [large body of work](#) focuses on stability, *e.g.*, [11], [12] are concerned with finite-time delay-dependent stability of discrete-time systems, [13] finds sufficient conditions for uniform stability of linear delay systems, [14] [characterizes stability and consensus conditions with homogeneous and heterogeneous feedback delays](#), and [15], [16] analyze consensus and error compensation for vehicular platoons. Another line of work deals with maximizing performance for structured controllers, *e.g.*, [17]–[19] [study \$\mathcal{H}_2\$ -norm minimization for time-delay network systems](#), [20] proposes a cyber-physical architecture with LQR for wide-area power systems, [21] develops a procedure for time-varying dead-time compensation by adapting the Filtered Smith Predictor, and [22] investigates sensor-and-processing selection for optimal estimation in star networks.

A more recent trend is optimizing the controller architecture. For large-scale systems, this means sparsifying the structure to enhance communication and scalability. This is achieved by introducing penalty terms to trade performance for controller complexity [23]–[30]. In particular, [29] proposes the *Regularization for Design*, addressing optimization of communication links, [while \[30\] investigates communication locality and its relation to control design within the System Level Synthesis framework](#).

Related work in optimization theory is concerned with minimization of distributed cost functions, which are only partially accessible at each agent. A large body of literature has been devoted to study suitable algorithms, a short list of which is represented by [31]–[38]. In particular, a line of work has been concerned specifically with the design of algorithms in the presence of communication delays, the main issues being related to convergence conditions. For example, [39]–[43] study consensus of multi-agent systems with additive or multiplicative time-delays under various network topologies and agent dynamics. This approach usually the communication network be given and focuses on the information exchange and processing by the agents from an optimization standpoint.

Addressed Problem. Even though both control design for delay-dependent dynamics and design of controller architectures are well-studied topics, it remains unclear how *network connectivity affects the closed-loop performance in the presence of architecture-dependent communication latency*. When the total available bandwidth does not increase with the size of the network [43] or when multi-hop communication is used among low-power devices [44], the number of active communication links may [affect such latency in non-negligible way](#). In this case,

This work has been partially supported by the Italian Ministry of Education, University and Research (MIUR) through the PRIN project no. 2017NS9FEY entitled “Realtime Control of 5G Wireless Networks”, and through the initiative “Departments of Excellence” (Law 232/2016), and by the US National Science Foundation (NSF) under Awards ECCS-1708906 and ECCS-1809833. Views and opinions expressed in this work are of the authors and may not reflect those of the funding institutions.

Luca Ballotta and Luca Schenato are with the Department of Information Engineering, University of Padova, 35131 Padova, Italy (e-mail: ballotta@dei.unipd.it; schenato@dei.unipd.it)

Mihailo R. Jovanović is with the Ming Hsieh Department of Electrical and Computer Engineering, University of Southern California, Los Angeles, CA 90089 USA (e-mail: mihailo@usc.edu)

it is important that the control design takes into account increase in delays when new communication links are introduced.

Such an approach is conceptually different from the approaches used in literature. On one hand, delay-aware control designs such as [14], [19] assume a fixed controller architecture and either target optimization of the feedback gains or evaluate stability with respect to gains and/or delays. On the other hand, architecture designs such as [27], [29] do not quantify the impact of architecture-dependent delays on performance, but explicitly force sparsity by adding a regularization term that penalizes controller complexity to delay-free performance metrics. In fact, while the fully connected architecture is avoided because of practical limitations, it is usually regarded as an upper bound for performance [1]. To the best of our knowledge, the only works where architecture-dependent delays are used to compute the performance metric are [44], [45], where the authors study how transmission power affects convergence rate of consensus.

We study class of static feedback policies in which control action is formed by utilizing delayed measurements from a limited number of nodes within a network. Impact of similar type of controller architectures on mean-square performance of delay-free stochastically forced consensus, synchronization, and vehicular formation networks has been studied in the literature [36], [46], and our objective is to understand influence of delays on performance trade-offs induced by such localized controller architectures relative to centralized ones. Identifying similar trade-offs within other classes of localized control policies (including System Level Synthesis) is a relevant open question which is outside the scope of the current study.

Original Contribution. We aim to bridge the two domains of delay-aware control and architecture design by quantifying how the latter affects performance under architecture-dependent communication delays. We address two key challenges. First, we focus on *optimal performance*, whereby *stability* is a prerequisite to control design needed to provide a bounded cost function. Hence, we derive stability conditions that are instrumental to an optimal control design problem. Second, we aim to identify the *optimal controller architecture* under delays and quantify fundamental performance trade-offs. Towards this goal, to circumvent the discrete nature of graphs, we work our way through two stages: first, we parametrize each architecture with a parameter n which characterizes both number of links and delay associated with that architecture, and show how to compute the optimal controller for a given n . We then compare the optimal performance obtained for different values of n , which allows us to fairly establish which architectures provide the best closed-loop performance. In contrast to [44], [45], we examine mean-square performance of stochastically forced networks, study generic delay functions, and address optimal design of feedback gains for different controller architectures.

Preview of Key Results. We utilize undirected graphs with single- and double-integrator agent dynamics to examine fundamental performance limitations in networked systems with architecture-dependent communication delays. By exploiting convexity of a minimum-variance control design problem with respect to the feedback gains, we demonstrate that the choice of controller architecture has profound impact on network

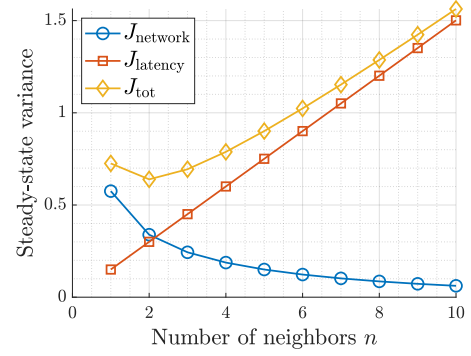


Fig. 1. Steady-state variance $J_{\text{tot}}(n)$ versus number of neighbors. The variance is the sum of two costs: $J_{\text{network}}(n)$ represents impact of control architecture, while $J_{\text{latency}}(n)$ is due to the delays affecting the dynamics.

TABLE I
OUTLINE OF THEORETICAL TOOLS (ITALIC FONT) AND TECHNICAL RESULTS (ROMAN FONT).

	Model	Stability	Variance
Cont. time (CT)	Single int. (III.1),(II.3)	<i>Scalar SDDEs [47]</i> Closed form (III.4)	<i>Scalar SDDEs [47]</i> Closed form (III.5)
	Double int. (III.7)–(II.4)	<i>Exponential polynomials [48]</i> <i>SDDEs [49], [50]</i> Implicit (III.10)	<i>SDDEs [50], time-scale separation [51]</i> Integral form (III.13) Approximated (III.14)
Disc. time (DT)	Single int. (VI.1),(II.3)	<i>Root locus [52]</i> Closed form (VI.3)	<i>Moment matching w/ Yule-Walker eqs. [53]</i> Recursive (E.2),(E.7)
	Double int. (VI.2)	<i>Jury criterion [54]</i> Closed form (D.4)	<i>Moment matching w/ Yule-Walker eqs. [53]</i> Closed form (E.18)

performance in the presence of delays. In particular, when the delays increase fast enough with the number of links, sparse topologies can outperform highly connected ones.

We show that the steady-state variance of a stochastically forced network, $J_{\text{tot}}(n)$, can be represented by a sum of two monotone functions of the number of neighbors n (Fig. 1),

$$J_{\text{tot}}(n) = J_{\text{network}}(n) + J_{\text{latency}}(n). \quad (\text{I.1})$$

Here, $J_{\text{network}}(n)$ quantifies impact of control architecture and $J_{\text{latency}}(n)$ determines influence of communication latency on network performance. While $J_{\text{network}}(n)$ decreases with n and is minimized by a fully-connected centralized architecture, $J_{\text{latency}}(n)$ increases with n . This demonstrates the presence of a fundamental trade-off: on one hand, feedback control takes advantage of dense topologies that enhance information sharing but, on the other hand, many communication links induce long delays which have negative effect on performance.

While (I.1) can be derived analytically for ring topology with continuous-time, single-integrator dynamics, our computational experiments show that a similar *centralized-decentralized trade-off* can be observed for general undirected topologies and with double-integrator and discrete-time agent dynamics. Furthermore, in some cases, decentralized architecture with nearest neighbor information exchange provides optimal performance.

Paper Outline. In Section II we describe models for communication and controller architecture and formulate the minimum-variance control design problem. While we

first utilize ring topology to provide analytical insight we also demonstrate that our framework can be extended to general undirected topologies; see Section IV-A. In Sections III–IV, we lay the ground for our main result. In Section III, we derive conditions for mean-square stability and compute the steady-state variance of continuous-time stochastically forced systems using Stochastic Delay Differential Equations (SDDEs). In Section IV, we prove that the control design problem is convex and in Section V we present our main results: by numerically computing the optimal controller gains, we show that the closed-loop performance is optimized by sparse architectures. Furthermore, we derive analytical expression (I.1) for continuous-time single-integrator dynamics which demonstrates that the minimizer is in general nontrivial. To address realistic wireless communication, we study discrete-time systems in Section VI and show that the fundamental behavior of the system does not change. Table I summarizes our technical results and the theoretical tools exploited throughout the paper. Apart from classical control techniques such as the Jury stability criterion, we also leverage more unconventional tools from mathematical literature, such as roots of exponential polynomials [48]. Concluding remarks are provided in Section VII.

II. PROBLEM SETUP

We consider an undirected network with N agents in which the state of the i th agent at time t is given by $\bar{x}_i(t) \in \mathbb{R}$ with the control input $u_i(t) \in \mathbb{R}$. For notational convenience, we introduce the aggregate state of the system $\bar{x}(t)$ and the aggregate control input $u(t)$ by stacking states and control inputs of each subsystem $\bar{x}_i(t)$ and $u_i(t)$, respectively.

Problem Statement. The agents aim to reach consensus towards a common state trajectory. The i th component of the vector $x(t) \doteq \Omega \bar{x}(t)$ represents the mismatch between the state of agent i and the average network state at time t [46], where

$$\Omega \doteq I_N - \frac{\mathbf{1}_N \mathbf{1}_N^\top}{N} \quad (\text{II.1})$$

and $\mathbf{1}_N \in \mathbb{R}^N$ is the vector of all ones, such that $\Omega \mathbf{1}_N = 0$.

Ring Topology. We focus on ring topology to obtain analytical insights about optimal control design and fundamental performance trade-offs in the presence of communication delays. While some of our notation is tailored to such topology (e.g., see equations (II.2) and (II.5)), in Section IV-A we discuss extension of the optimal control design to generic undirected networks and complement these developments with computational experiments in Section V.

Assumption 1 (Communication model). *Data are exchanged through a shared wireless channel in a symmetric fashion. Agent i receives state measurements from n pairs of agents, where both agents in each such pair are at equal distance ℓ from i . In what follows, without loss of generality, we assume that such n agent pairs coincide with the $2n$ closest agents in ring topology, and that each pair is at distance $\ell = 1, \dots, n < N/2$. For example, $n = 1$ corresponds to nearest-neighbor interaction and $n = \lfloor (N-1)/2 \rfloor$ to all-to-all communication. All*

measurements are received with delay $\tau_n \doteq f(n)$ where $f(\cdot)$ is a positive increasing sequence.

Remark 1 (Architecture parametrization). *Parameter n will play a crucial role throughout our discussion. In particular, we will use it to (i) evaluate the optimal performance that can be attained for a given budget of communication links; and to (ii) compare optimal performance of different control architectures. In the first part of the paper, we examine circular formations and n represents how many neighbor pairs communicate with each agent. For general undirected networks, n determines the number of communication hops for each agent. In general, the parameter n characterizes sparsity of a controller architecture: sparse controllers correspond to small n whereas highly connected ones correspond to large n .*

Feedback Control. Agent i uses the received information to compute the state mismatches $y_{i,\ell\pm}(t)$ relative to its neighbors,

$$y_{i,\ell\pm}(t) = \begin{cases} \bar{x}_i(t) - \bar{x}_{i\pm\ell}(t), & 0 < i \pm \ell \leq N \\ \bar{x}_i(t) - \bar{x}_{i\pm\ell \mp N}(t), & \text{otherwise,} \end{cases} \quad (\text{II.2})$$

and the proportional control input is given by

$$u_{P,i}(t) = - \sum_{\ell=1}^n k_\ell (y_{i,\ell+}(t - \tau_n) + y_{i,\ell-}(t - \tau_n)), \quad (\text{II.3})$$

where measurements are delayed according to Assumption 1.

For networks with double integrator agents, the control input $u_i(t)$ may also include a derivative term,

$$u_i(t) = \eta u_{P,i}(t) - \eta \frac{d\bar{x}_i(t)}{dt} = \eta u_{P,i}(t) - \eta \frac{dx_i(t)}{dt}. \quad (\text{II.4})$$

The derivative term in (II.4) is delay free because it only requires measurements coming from the agent itself, which we assume to be available instantaneously. The proportional input can be compactly written as $u_P(t) = -K\bar{x}(t - \tau_n) = -Kx(t - \tau_n)$. With ring topology, the feedback gain matrix is determined by

$$K = \text{circ} \left(\sum_{\ell=1}^n k_\ell, -k_1, \dots, -k_n, 0, \dots, 0, -k_n, \dots, -k_1 \right), \quad (\text{II.5})$$

where $\text{circ}(a_1, \dots, a_n)$ denotes the circulant matrix in $\mathbb{R}^{n \times n}$ with elements a_1, \dots, a_n in the first row.

Problem 1. *Design the feedback gains in order to minimize the steady-state variance of the consensus error,*

$$P \text{ control:} \quad \underset{K}{\operatorname{argmin}} \sigma^2(K), \quad (\text{II.6a})$$

$$PD \text{ control:} \quad \underset{\eta, K}{\operatorname{argmin}} \sigma^2(\eta, K), \quad (\text{II.6b})$$

where

$$\sigma^2 \doteq \lim_{t \rightarrow +\infty} \mathbb{E} [\|x(t)\|^2] \quad (\text{II.7})$$

and w.l.o.g. we assume $\mathbb{E}[x(\cdot)] \equiv \mathbb{E}[x(0)] = 0$.

III. CONTINUOUS-TIME AGENT DYNAMICS

We now examine continuous-time networks with single- (Section III-A) and double-integrator (Section III-B) agent

dynamics, derive conditions for mean-square stability, and compute the steady-state variance of a stochastically forced system. These developments are instrumental for the formulation of the control design problem which is used to compare different control architectures. In the optimal control problem, the steady-state variance determines the objective function and stability conditions represent constraints. While we first formulate and solve the problem for continuous-time dynamics, our results also hold for discrete-time systems; see Section VI. Also, all results in this section hold for generic undirected topologies.

A. Single Integrator Model

The dynamics of the i th agent are described by the first-order differential equation driven by standard Brownian noise $\bar{w}_i(\cdot)$,

$$d\bar{x}_i(t) = u_{P,i}(t)dt + d\bar{w}_i(t). \quad (\text{III.1})$$

The network error dynamics are

$$dx(t) = -Kx(t - \tau_n)dt + dw(t), \quad (\text{III.2})$$

where the process noise is given by $dw(t) \sim \mathcal{N}(0, \Omega\Omega^\top dt)$. Exploiting symmetry of the matrix K , we employ the change of variables $x(t) = T\tilde{x}(t)$, with $K = T\Lambda T^\top$, to obtain N decoupled scalar subsystems with state $\tilde{x}_j(t)$, $j = 1, \dots, N$,

$$d\tilde{x}_j(t) = -\lambda_j\tilde{x}_j(t - \tau_n)dt + d\tilde{w}_j(t), \quad (\text{III.3})$$

where λ_j is the j th eigenvalue of K . The subsystem with $\lambda_1 = 0$ has trivial dynamics, i.e., $d\tilde{x}_1(t) \equiv 0$, with initial condition $\tilde{x}_1(0) = 0$ by construction. For $j \neq 1$, subsystem (III.3) is a single integrator driven by standard Brownian noise.

Stability Analysis. Mean-square stability of scalar stochastic differential equations of the form (III.3) has been addressed in the literature. We build on the classical result in [47] to characterize consensus stability for the multi-agent formation.

Proposition 1 (Stability of CT single integrators). *The network error $x(t)$ is mean-square stable if and only if*

$$\lambda_j \in \left(0, \frac{\pi}{2\tau_n}\right), \quad j = 2, \dots, N. \quad (\text{III.4})$$

In this case, $x(t)$ is a Gaussian process and its steady-state variance is determined by

$$\sigma^2(K) = \sum_{j=2}^N \sigma_I^2(\lambda_j), \quad \sigma_I^2(\lambda_j) = \frac{1 + \sin(\lambda_j\tau_n)}{2\lambda_j \cos(\lambda_j\tau_n)}, \quad (\text{III.5})$$

where $\sigma_I^2(\lambda_j)$ is the variance of the trivial solution of (III.3).

Sketch of Proof: In view of decoupling, stability of (III.2) amounts to stability of all subsystems (III.3), $j = 1, \dots, N$, with the variances of $x(t)$ and $\tilde{x}(t)$ being equal. Condition (III.4) and expression (III.5) were derived in [47]. ■

While the variance of delay-free systems is bounded for any positive eigenvalues $\lambda_2, \dots, \lambda_N$, the presence of delay constrains a stabilizing control according to (III.4). In fact, longer delays τ_n induce smaller upper bounds on the eigenvalues.

The following result will turn useful in the control design.

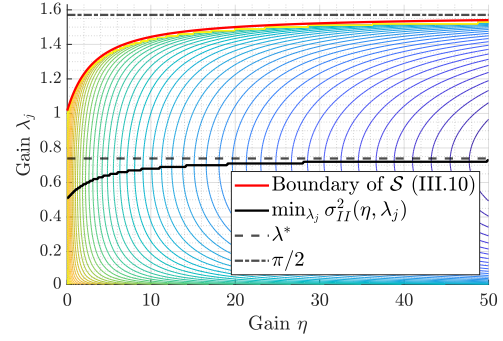


Fig. 2. Level curves of the steady-state variance for the continuous-time double integrator (III.9) and points of minimum with fixed derivative gain.

Corollary 1. *Let λ satisfy (III.4). Then the function $\sigma_I^2(\lambda)$ is strictly convex and the minimizer λ^* is determined by*

$$\lambda^* = \frac{\beta^*}{\tau_n}, \quad \beta^* = \cos \beta^*. \quad (\text{III.6})$$

Proof: Follows from computations over the derivatives of $\sigma_I^2(\cdot)$. See Appendices A-B in the preprint [55]. ■

B. Double Integrator Model

We now examine networks in which each agent obeys a second-order dynamics with the PD control input (II.4):

$$\frac{d^2\bar{x}_i(t)}{dt^2} = u_i(t) + \frac{d\bar{w}_i(t)}{dt}. \quad (\text{III.7})$$

For simplicity, we normalize the delay by rescaling (III.7),

$$\bar{x}_i(\cdot) \leftarrow \bar{x}_i(\tau_n \cdot), \quad \eta \leftarrow \tau_n \eta, \quad k_\ell \leftarrow \tau_n k_\ell, \quad \bar{w}_i(\cdot) \leftarrow \tau_n \bar{w}_i(\cdot), \quad (\text{III.8})$$

Stacking the agent errors and their derivatives in the formation vector, the error dynamics can be decoupled as before, yielding

$$\frac{d^2\tilde{x}_j(t)}{dt^2} = -\eta \frac{d\tilde{x}_j(t)}{dt} - \eta \lambda_j \tilde{x}_j(t - 1) + \frac{d\tilde{w}_j(t)}{dt}. \quad (\text{III.9})$$

Stability Analysis. We have the following result.

Proposition 2 (Stability of CT double integrators). *The network error $x(t)$ is mean-square stable if*

$$\lambda_j \in \left(0, \frac{\beta}{\sin \beta}\right), \quad \eta = \beta \tan \beta, \quad \beta \in \left(0, \frac{\pi}{2}\right), \quad j = 2, \dots, N. \quad (\text{III.10})$$

Condition (III.10) can be equivalently written as

$$(\eta, \lambda_j) \in \mathcal{S} \doteq \{(\eta, \lambda_j) \in \mathbb{R}_+^2 : \lambda_j < \phi(\eta)\}, \quad j = 2, \dots, N, \quad (\text{III.11})$$

where the implicit function $\phi(\cdot)$ is concave increasing and

$$\phi(0) = 1, \quad \lim_{\eta \rightarrow +\infty} \phi(\eta) = \frac{\pi}{2}. \quad (\text{III.12})$$

If $\exists j \neq 1 : (\eta, \lambda_j) \notin \bar{\mathcal{S}}$, the system is mean-square unstable.

Proof: See Appendix A. ■

Similar to the single-integrator case, Proposition 2 states that the presence of delay requires more restrictive conditions than positive gains. In words, the system is stable if the instantaneous component of the control input in (II.4) is sufficiently “strong”

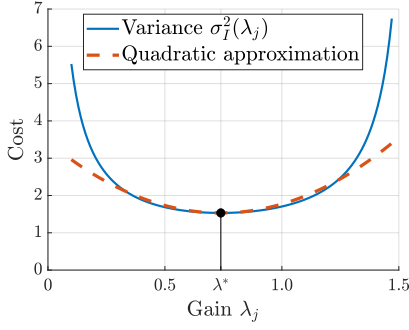


Fig. 3. Exact variance function (III.5) and its quadratic approximation.

compared to the delayed one. The steady-state variance of $\hat{x}_j(t)$ for $j \neq 1$ can be computed using [50, Section 4],

$$\sigma_H^2(\eta, \lambda_j) = \frac{1}{2\pi} \int_{-\infty}^{+\infty} \frac{d\omega}{|-\omega^2 + j\eta\omega + \eta\lambda_j e^{-j\omega}|^2}, \quad (\text{III.13})$$

and $\sigma^2 = \sigma^2(\eta, K) = \sum_{j=2}^N \sigma_H^2(\eta, \lambda_j)$. A graphical illustration of the level curves of $\sigma_H^2(\eta, \lambda_j)$ is provided in Fig. 2.

Model Approximation. As shown in Appendix B, when the feedback gain η is sufficiently high, separation of time scales allows us to approximate (III.9) with the first-order dynamics,

$$d\tilde{x}_j(t) = -\lambda_j \tilde{x}_j(t-1)dt + dn(t), \quad (\text{III.14})$$

where the variance of Brownian motion $n(t)$ is inversely proportional to η . In words, when the damping is high enough, the derivative of $\tilde{x}_j(t)$ converges to zero much faster than $\tilde{x}_j(t)$, which represents the dominant component of the dynamics. Utility of this approximation is illustrated in Fig. 2: with fixed $\bar{\eta}$, the point of minimum of the corresponding 1D variance curve, *i.e.*, $\arg\min_{\lambda_j} \sigma_H^2(\bar{\eta}, \lambda_j)$ (solid black line), approaches the minimizer λ^* of the single integrator model (dashed black, see Corollary 1) with increase of $\bar{\eta}$. We also note that the variance decreases with η .

IV. CONTROL DESIGN

Single Integrator Model. For system (III.2) Problem 1 amounts to

$$k_1^*, \dots, k_n^* = \arg\min_{\{k_\ell\}_{\ell=1}^n} \sigma^2(K), \quad (\text{IV.1})$$

and parameterization (III.3) allows to rewrite it as

$$k_1^*, \dots, k_n^* = \arg\min_{\{k_\ell\}_{\ell=1}^n} \sum_{j=2}^N \sigma_I^2(\lambda_j), \quad (\text{IV.2})$$

with stability condition given by (III.4). Linear dependence of the eigenvalues of K on the feedback gains [56] and Corollary 1 guarantee convexity of optimization problem (IV.2). Thus, the optimal feedback gains can be computed efficiently.

To make analytical progress and gain intuition, we also consider the following approximation of (IV.2),

$$\tilde{k}_1^*, \dots, \tilde{k}_n^* = \arg\min_{\{k_\ell\}_{\ell=1}^n} \sum_{j=2}^N (\lambda_j - \lambda^*)^2, \quad (\text{IV.3})$$

which squeezes the spectrum of K about the “optimal” eigenvalue λ^* . The variance $\sigma_I^2(\cdot)$ can be approximated with a quadratic function around its minimum because it is strictly convex, differentiable in the stability region, and it blows up at the boundaries $\{0, \pi/2\}$, see Fig. 3.

Proposition 3 (Near-optimal proportional control). *The solution of problem (IV.3) is determined by*

$$\tilde{k}_\ell^* \equiv \tilde{k}^* \doteq \frac{\lambda^*}{2n+1}.$$

Proof: The result follows by applying properties of the DFT to (IV.3); see Appendices C-D in [55] for details. ■

Proposition 3 shows that spatially-constant feedback gains provide good performance even when spatially-varying feedback gains are allowed. According to Corollary 1, the suboptimal gain \tilde{k}^* decreases with the delay τ_n and with the number of agents involved in the feedback loops, thereby reflecting benefits of communication.

Double Integrator Model. Approximation (III.14) and Fig. 2 show that, for sufficiently large η , the variance of the double-integrator subsystem (III.9) has structure similar to the single integrator, *i.e.*, $\sigma_H^2(\eta, \lambda_j) \approx c\sigma_I^2(\lambda_j)$ for some “small” $c > 0$. Thus, we approximate the control design (II.6b) as

$$\tilde{\eta}^*, \arg\min_{\{k_\ell\}_{\ell=1}^n} \sum_{j=2}^N \sigma_I^2(\lambda_j), \quad (\text{IV.4})$$

where $\tilde{\eta}^*$ is chosen beforehand so that the time-scale separation argument provides a reasonable approximation (III.14). In particular, the optimization problem for proportional feedback gains in (IV.4) coincides with the control design for single integrators (IV.2), with the exception that the stability condition is now given by $\lambda_j < \phi(\tilde{\eta}^*)$, $j = 2, \dots, N$; see (III.11).

Remark 2 (Convexity enables comparison). *Convexity of the optimal control design problems (IV.2)–(IV.4) enables both efficient numerical computations of the optimal feedback gains for given n and fair comparison of the best achievable performance for different values of n .*

Remark 3 (Gain scaling). *The optimal feedback gains $\{k_\ell^*\}_{\ell=1}^n$ and $\tilde{\eta}^*$ are to be scaled by $1/\tau_n$ according to (III.8).*

Remark 4 (Optimal design for double integrators). *Local minimizer of the original problem approximated by (IV.4) can be solved using the gradient-based method proposed in [17]. However, this approach has no guarantees of global optimality, and its computational complexity is impractical for large-scale systems. In contrast, convex approximation (IV.4) draws a parallel to the optimal design for the single-integrator model and provides insight into a centralized-decentralized trade-off.*

A. General Symmetric Network Topology

Even though we utilized ring topology to derive analytical results (see Section V-A), the control design can be extended to general undirected networks with symmetric feedback gain matrices K . For the single integrator model, this reads

$$K^* = \arg\min_K \sigma^2(K). \quad (\text{IV.5})$$

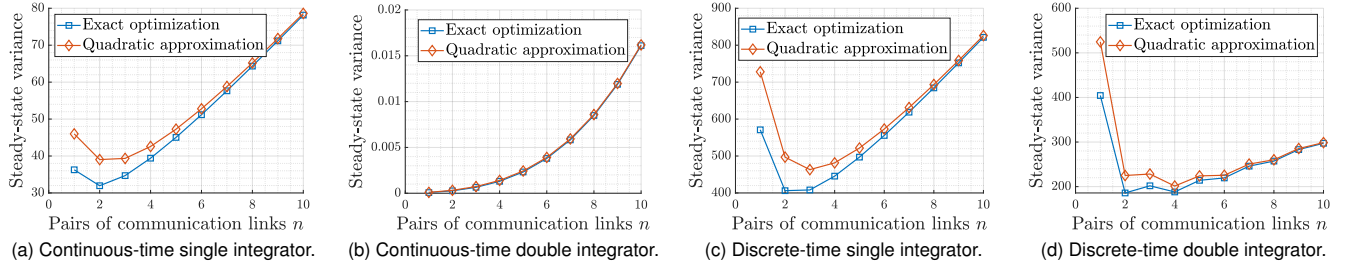


Fig. 4. Optimal and suboptimal steady-state scalar variances with linear delay increase for different agent dynamics.

The steady-state network error variance $\sigma^2(K)$ is a convex function if and only if $\sigma_l^2(\lambda_j)$ is convex [57], which is proved in Corollary 1 for continuous-time and in Appendix E for discrete-time systems. The optimal gains can then be found numerically via gradient-based methods, where gradients of the eigenvalues can be computed using analytical [58], [59] or numerical [60] methods. On the other hand, the derivative feedback gain in $\sigma_H^2(\eta, \lambda_j)$ prevents us from establishing convexity for second-order systems in general. However, if $\sigma_H^2(\eta, \lambda_j)$ is convex in each coordinate¹, the design problem can be solved by alternatively optimizing proportional and derivative gains and the centralized-decentralized trade-off can be studied irrespective of the particular topology.

V. THE CENTRALIZED-DISTRIBUTED TRADE-OFF

In the previous sections we formulated the optimal control problem for a given controller architecture (*i.e.*, the number of links) parametrized by n and showed how to compute minimum-variance objective function and the corresponding constraints. In this section, we present our main result: we solve the optimal control problem for each n and compare the best achievable closed-loop performance with different control architectures.² For delays that increase linearly with n , *i.e.*, $f(n) \propto n$, we demonstrate that distributed controllers with few communication links outperform controllers with larger number of communication links.

Figure 4a shows the steady-state variances obtained with single-integrator dynamics (IV.1) and the quadratic approximation (IV.3) for ring topology with $N = 50$ nodes. The best performance is achieved for a sparse architecture with $n = 2$ in which each agent communicates with the two closest pairs of neighboring nodes. This should be compared and contrasted to nearest-neighbor and all-to-all communication topologies which induce higher closed-loop variances. Thus, the advantage of introducing additional communication links diminishes beyond a certain threshold because of communication delays.

Figure 4b shows that the use of approximation (IV.4) with $\tilde{\eta}^* = 70$ identifies nearest-neighbor information exchange as the near-optimal architecture for a double-integrator model with ring topology. This can be explained by noting that the variance of the process noise $n(t)$ in the reduced model (III.14) is proportional to $1/\eta$ and thereby to τ_n , according to (III.8), making the variance scale with the delay.

¹This can be checked for discrete-time double integrators, see Appendix E.

²Recall that small (large) values of n mean sparse (dense) architectures.

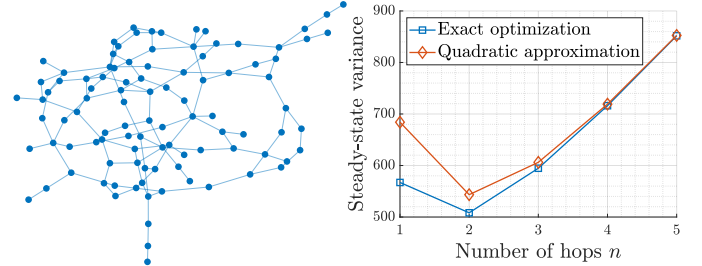


Fig. 5. Network topology and its optimal closed-loop variance.

Figures 4c–4d show the results obtained by solving the optimal control problem for discrete-time dynamics. The oscillations about the minimum in Fig. 4d are compatible with the investigated centralized-decentralized trade-off (I.1): in general, the sum of two monotone functions does not have a unique local minimum. Details about discrete-time systems are deferred to Section VI. Interestingly, double integrators with continuous- and discrete-time dynamics exhibit very different trade-off curves, whereby performance monotonically deteriorates for the former and oscillates for the latter. While a clear interpretation is difficult because there is no explicit expression of the variance as a function of n , one possible explanation might be the first-order approximation used to compute gains in the continuous-time case.

Finally, Fig. 5 shows the optimization results for a random graph topology with discrete-time single integrator agents. Here, n denotes the number of communication hops in the “original” network, shown in Fig. 5: as n increases, each agent can first communicate with its nearest neighbors, then with its neighbors’ neighbors, and so on. For a control architecture that utilizes different feedback gains for each communication link (*i.e.*, we only require $K = K^\top$) we demonstrate that, in this case, two communication hops provide optimal closed-loop performance.

Additional computational experiments performed with different rates $f(\cdot)$ show that the optimal number of links increases for slower rates: for example, the optimal number of links is larger for $f(n) = \sqrt{n}$ than for $f(n) = n$. These results are not reported because of space limitations.

A. Ring Topology: Analytical Insight into the Trade-Off

For a ring topology with continuous-time single-integrator agent dynamics, a centralized-decentralized trade-off can be

explicitly quantified. By utilizing Proposition 3 to compute the feedback gains, the objective function can be factorized as

$$\sigma^2 = \underbrace{f(n)}_{\tilde{J}_{\text{latency}}(n)} \cdot \underbrace{\sum_{j=2}^N \tilde{C}_j^*(n)}_{\tilde{J}_{\text{network}}(n)}, \quad (\text{V.1})$$

where $\sigma_I^2(\tilde{\lambda}_j^*) = \tilde{C}_j^*(n)\tau_n$ and $\tilde{C}_j^*(n)$ only depends on n and can be computed exactly; see Appendix C. This holds because the suboptimal eigenvalues can be expressed as $\tilde{\lambda}_j^* = \tilde{c}_j^*(n)\lambda^*$ (cf. Proposition 3). Such a decomposition can be interpreted as a decoupling of the impact of network ($\tilde{c}_j^*(n)$) and latency (λ^*) effects on the control design. By inspection, it can be seen that $\tilde{J}_{\text{network}}(n)$ is a decreasing function of n and that $\tilde{J}_{\text{latency}}(n)$ is determined by $f(n)$. Furthermore, when $f(\cdot)$ is sublinear, the above expression can be equivalently written in form (I.1),

$$\sigma^2 = \underbrace{f(n)}_{\tilde{J}_{\text{latency}}(n)} \cdot \underbrace{\sum_{j=2}^N (\tilde{C}_j^*(n) - C^*)}_{\tilde{J}_{\text{network}}(n)} + \underbrace{(N-1)C^*f(n)}_{\tilde{J}_{\text{latency}}(n)}, \quad (\text{V.2})$$

where $\sigma_I^2(\lambda^*) = C^*\tau_n$ is the optimal variance according to (III.5) and Corollary 1. Indeed, the summation decreases with superlinear rate, so that $\tilde{J}_{\text{network}}(n)$ is a decreasing sequence. The terms in $\tilde{J}_{\text{network}}(n)$, each associated with a decoupled subsystem (III.3), illustrate benefits of communication: as n increases, the eigenvalues of K have more degrees of freedom and can squeeze more tightly about λ^* , reducing performance gaps between subsystems and theoretical optimum. We note that $\tilde{J}_{\text{network}}(n)$ vanishes for the fully connected architecture.

Even though analogous expressions could not be obtained for other dynamics, the curves in Fig. 4 exhibit trade-offs which are consistent with the above analysis.

VI. DISCRETE-TIME AGENT DYNAMICS

We now consider discrete-time agent dynamics to illustrate that the afore-established fundamental trade-offs hold in this case as well. In what follows, we denote time instants by $\{k\}_{k \in \mathbb{N}} \doteq \{kT\}_{k \in \mathbb{N}}$, T being the sampling time. Similarly, we re-define the delay as the number of delay steps $\tau_n \doteq \lceil \tau_n/T_s \rceil$.

Agent Models. The discrete-time versions of the agent dynamics considered in Section III are given by

$$\bar{x}_i(k+1) = \bar{x}_i(k) + u_{P,i}(k) + \bar{w}_i(k), \quad (\text{VI.1})$$

for the single-integrator model, with $\bar{w}_i(\cdot) \sim \mathcal{N}(0, 1)$, and

$$\begin{aligned} \bar{x}_i(k+1) &= \bar{x}_i(k) + \bar{z}_i(k) \\ \bar{z}_i(k+1) &= (1-\eta)\bar{z}_i(k) + \eta u_{P,i}(k) + \bar{w}_i(k), \end{aligned} \quad (\text{VI.2})$$

for the double-integrator model, with $u_{P,i}(k)$ defined in (II.3).

Stability Analysis. The formation error dynamics can be decoupled analogously to the continuous-time models. The decoupled subsystems are asymptotically stable if and only if all the roots of their associated characteristic polynomials lie inside the unit circle in the complex plane.

In general, given a delay τ_n , stability conditions with respect to the control gains can be derived in the form of polynomial

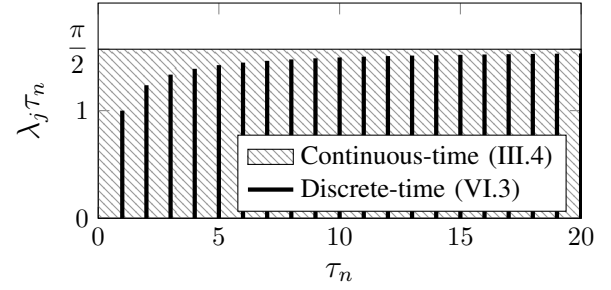


Fig. 6. Stability regions of decoupled single integrators.

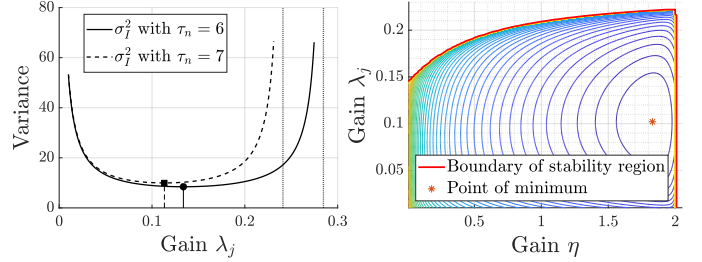


Fig. 7. Typical profiles of the steady-state variance for decoupled discrete-time single integrators (left) and double integrators (right).

inequalities through the Jury criterion. For the single-integrator case, one simple condition can be computed analytically.

Proposition 4 (Stability of DC single integrators). *The network error $x(t)$ is mean-square stable if and only if*

$$\lambda_j \in \left(0, 2 \sin \left(\frac{\pi}{2} \frac{1}{2\tau_n + 1} \right) \right), \quad j = 2, \dots, N. \quad (\text{VI.3})$$

The upper bound in (VI.3) approaches its continuous-time counterpart (III.4) from below as the delay steps tend to infinity (see Fig. 6). A discussion on general stability conditions and the proof of Proposition 4 are provided in Appendix D. The basic argument is the same as for the continuous-time case.

Performance Evaluation. With fixed parameters, the steady-state variance of each decoupled subsystem can be computed numerically via the Wiener–Khinchine formula. Also, for any given value of τ_n , a closed-form expression of the variance can be obtained via moment matching through a recursive formula, see Appendix E. Such closed-form expressions have been used for our computational experiments illustrated in Fig. 4. Figure 7 shows the typical profiles of the variance function for decoupled subsystems with single- and double-integrator dynamics (see (D.1) and (D.3) in Appendix E, respectively).

VII. CONCLUSION AND FUTURE RESEARCH

We study minimum-variance control design problem for undirected networks with both continuous- and discrete-time agent dynamics in the presence of communication delays. When feedback delays increase with the number of communication links, we identify fundamental performance trade-offs and show that distributed control architectures can offer superior performance to centralized ones that utilize all-to-all information exchange. Our hope is to pave the way to a new body of research which will enable control design with a deeper

understanding of the fundamental behavior and limitations of large-scale wireless network systems. Future work will focus on extending our results to other classes of control problems which include more complex system dynamics and communication models, more realistic information about structure of delays in a distributed scenario, as well as different cost functions.

REFERENCES

- [1] M. R. Jovanović and N. K. Dhingra, "Controller architectures: Tradeoffs between performance and structure," *Eur. J. Control*, vol. 30, pp. 76–91, 2016.
- [2] A. Nedić, A. Olshevsky, and M. G. Rabbat, "Network topology and communication-computation tradeoffs in decentralized optimization," *Proc. of the IEEE*, vol. 106, no. 5, pp. 953–976, 2018.
- [3] A. Biral, M. Centenaro, A. Zanella, L. Vangelista, and M. Zorzi, "The challenges of mMTC massive access in wireless cellular networks," *Digital Communications and Networks*, vol. 1, no. 1, pp. 1–19, 2015.
- [4] S. Li, L. Da Xu, and S. Zhao, "5G internet of things: A survey," *J. of Industrial Information Integration*, vol. 10, pp. 1–9, 2018.
- [5] A. Suleiman, Z. Zhang, L. Carlone, S. Karaman, and V. Sze, "Navion: A 2-mw fully integrated real-time visual-inertial odometry accelerator for autonomous navigation of nano drones," *IEEE J. Solid-State Circuits*, vol. 54, no. 4, pp. 1106–1119, 2019.
- [6] NVIDIA, "Nvidia jetson nano datasheet," 2020.
- [7] P. Warden and D. Situnayake, *TinyML: Machine Learning with TensorFlow Lite on Arduino and Ultra-Low-Power Microcontrollers*. O'Reilly Media, 2019.
- [8] W. Shi, S. Zhou, Z. Niu, M. Jiang, and L. Geng, "Joint device scheduling and resource allocation for latency constrained wireless federated learning," *IEEE Trans. Wireless Commun.*, vol. 20, no. 1, pp. 453–467, 2020.
- [9] W. Shi, J. Cao, Q. Zhang, Y. Li, and L. Xu, "Edge computing: Vision and challenges," *IEEE Internet Things J.*, vol. 3, no. 5, pp. 637–646, 2016.
- [10] S. Yi, C. Li, and Q. Li, "A survey of fog computing: concepts, applications and issues," in *Proc. ACM WRKSH Mobile Big Data*, 2015, pp. 37–42.
- [11] H. Ren, G. Zong, L. Hou, and Y. Yang, "Finite-time resilient decentralized control for interconnected impulsive switched systems with neutral delay," *ISA Trans.*, vol. 67, pp. 19–29, 2017.
- [12] S. Sun, H. Zhang, W. Li, and Y. Wang, "Time-varying delay-dependent finite-time boundedness with \mathcal{H}_∞ performance for markovian jump neural networks with state and input constraints," *Neurocomputing*, vol. 423, pp. 419–426, 2021.
- [13] L. Berežansky, J. Diblík, Z. Svoboda, and Z. Šmarda, "Simple uniform exponential stability conditions for a system of linear delay differential equations," *Appl. Math. Comput.*, vol. 250, pp. 605 – 614, 2015.
- [14] U. Münz, A. Papachristodoulou, and F. Allgöwer, "Delay robustness in consensus problems," *Automatica*, vol. 46, no. 8, pp. 1252–1265, 2010.
- [15] H. Chehardoli and A. Ghasemi, "Formation control of longitudinal vehicular platoons under generic network topology with heterogeneous time delays," *J. Vib. Control*, vol. 25, no. 3, pp. 655–665, 2019.
- [16] F. de Oliveira Souza, L. A. B. Torres, L. A. Mozelli, and A. A. Neto, "Stability and formation error of homogeneous vehicular platoons with communication time delays," *IEEE Trans. Intell. Transp. Syst.*, vol. 21, no. 10, pp. 4338–4349, 2020.
- [17] M. A. Gomez, A. V. Egorov, S. Mondié, and W. Michiels, "Optimization of the \mathcal{H}_2 norm for single-delay systems, with application to control design and model approximation," *IEEE Trans. Autom. Control*, vol. 64, no. 2, pp. 804–811, 2019.
- [18] W. Michiels, G. Hilhorst, G. Pipeleers, and J. Swevers, *Model Order Reduction for Time-Delay Systems, with Application to Fixed-Order \mathcal{H}_2 Optimal Controller Design*. Springer International Publishing, 2016, pp. 45–66.
- [19] S. Dezfoulian, Y. Ghaedsharaf, and N. Motee, "On performance of time-delay linear consensus networks with directed interconnection topologies," in *Proc. ACC*, 2018, pp. 4177–4182.
- [20] D. Soudbakhsh, A. Chakraborty, and A. M. Annaswamy, "A delay-aware cyber-physical architecture for wide-area control of power systems," *Control Engineering Practice*, vol. 60, pp. 171–182, 2017.
- [21] M. M. Morato and J. E. Normey-Rico, "A novel unified method for time-varying dead-time compensation," *ISA Trans.*, vol. 108, pp. 78–95, 2021.
- [22] L. Ballotta, L. Schenato, and L. Carlone, "Computation-communication trade-offs and sensor selection in real-time estimation for processing networks," *IEEE Trans. Netw. Sci. Eng.*, vol. 7, no. 4, pp. 2952–2965, 2020.
- [23] F. Lin, M. Fardad, and M. R. Jovanović, "Design of optimal sparse feedback gains via the alternating direction method of multipliers," *IEEE Trans. Autom. Control*, vol. 58, no. 9, pp. 2426–2431, 2013.
- [24] F. Dörfler, M. R. Jovanović, M. Chertkov, and F. Bullo, "Sparsity-promoting optimal wide-area control of power networks," *IEEE Trans. Power Syst.*, vol. 29, no. 5, pp. 2281–2291, 2014.
- [25] F. Lian, A. Chakraborty, and A. Duel-Hallen, "Game-theoretic multi-agent control and network cost allocation under communication constraints," *IEEE J. Sel. Areas Commun.*, vol. 35, no. 2, pp. 330–340, 2017.
- [26] P. R. Massenio, G. Rizzello, D. Naso, F. L. Lewis, and A. Davoudi, "Data-driven optimal structured control for unknown symmetric systems," in *IEEE 16th Int. Conf. on Autom. Sci. Eng.*, 2020, pp. 179–184.
- [27] N. Matni, "Communication delay co-design in \mathcal{H}_2 -distributed control using atomic norm minimization," *IEEE Control Netw. Syst.*, vol. 4, no. 2, pp. 267–278, 2017.
- [28] M. S. Bahavarnia and N. Motee, "Sparse memoryless LQR design for uncertain linear time-delay systems," *Proc. 20th IFAC World Congress*, vol. 50, no. 1, pp. 10395–10400, 2017.
- [29] N. Matni and V. Chandrasekaran, "Regularization for design," *IEEE Trans. Autom. Control*, vol. 61, no. 12, pp. 3991–4006, 2016.
- [30] J. Anderson, J. C. Doyle, S. H. Low, and N. Matni, "System level synthesis," *Annual Reviews in Control*, vol. 47, pp. 364–393, 2019.
- [31] T. Chen, Q. Ling, and G. B. Giannakis, "An online convex optimization approach to proactive network resource allocation," *IEEE Trans. Signal Process.*, vol. 65, no. 24, pp. 6350–6364, 2017.
- [32] L. Xiao, S. Boyd, and S.-J. Kim, "Distributed average consensus with least-mean-square deviation," *J. Parallel Distrib. Comput.*, vol. 67, no. 1, pp. 33–46, 2007.
- [33] S. Shahrampour and A. Jadbabaie, "Distributed online optimization in dynamic environments using mirror descent," *IEEE Trans. Autom. Control*, vol. 63, no. 3, pp. 714–725, 2018.
- [34] T. Tatarenko and B. Touri, "Non-convex distributed optimization," *IEEE Trans. Autom. Control*, vol. 62, no. 8, pp. 3744–3757, 2017.
- [35] P. Di Lorenzo and G. Scutari, "Distributed nonconvex optimization over time-varying networks," in *Proc. IEEE ICASSP*, 2016, pp. 4124–4128.
- [36] M. Fardad, F. Lin, and M. R. Jovanović, "Design of optimal sparse interconnection graphs for synchronization of oscillator networks," *IEEE Trans. Automat. Control*, vol. 59, no. 9, pp. 2457–2462, 2014.
- [37] S. Hassan-Moghaddam and M. R. Jovanović, "Topology design for stochastically-forced consensus networks," *IEEE Trans. Control Netw. Syst.*, vol. 5, no. 3, pp. 1075–1086, 2018.
- [38] N. K. Dhingra, S. Z. Khong, and M. R. Jovanović, "The proximal augmented Lagrangian method for nonsmooth composite optimization," *IEEE Trans. Automat. Control*, vol. 64, no. 7, pp. 2861–2868, 2019.
- [39] K. I. Tsianos and M. G. Rabbat, "Distributed consensus and optimization under communication delays," in *Proc. Allerton Conf. Commun., Control, Comput.*, 2011, pp. 974–982.
- [40] C. N. Hadjicostis and T. Charalambous, "Average consensus in the presence of delays in directed graph topologies," *IEEE Trans. Autom. Control*, vol. 59, no. 3, pp. 763–768, 2014.
- [41] X. Zong, T. Li, G. Yin, L. Y. Wang, and J.-F. Zhang, "Stochastic consentability of linear systems with time delays and multiplicative noises," *IEEE Trans. Autom. Control*, vol. 63, no. 4, pp. 1059–1074, 2018.
- [42] X. Zong, T. Li, and J.-F. Zhang, "Consensus conditions of continuous-time multi-agent systems with time-delays and measurement noises," *Automatica*, vol. 99, pp. 412–419, 2019.
- [43] E. Garcia, Y. Cao, and D. W. Casbeer, "Periodic event-triggered synchronization of linear multi-agent systems with communication delays," *IEEE Trans. Autom. Control*, vol. 62, no. 1, pp. 366–371, 2016.
- [44] S. Vanka, V. Gupta, and M. Haenggi, "Power-delay analysis of consensus algorithms on wireless networks with interference," *Int. J. Syst. Control Commun.*, vol. 2, no. 1–3, pp. 256–274, 2010.
- [45] S. Vanka, M. Haenggi, and V. Gupta, "Convergence speed of the consensus algorithm with interference and sparse long-range connectivity," *IEEE J. Sel. Top. Signal Process.*, vol. 5, no. 4, pp. 855–865, 2011.
- [46] B. Bamieh, M. R. Jovanović, P. Mitra, and S. Patterson, "Coherence in large-scale networks: dimension dependent limitations of local feedback," *IEEE Trans. Automat. Control*, vol. 57, no. 9, pp. 2235–2249, 2012.
- [47] U. Küchler and B. Mensch, "Langevins stochastic differential equation extended by a time-delayed term," *Stochastics and Stochastic Reports*, vol. 40, no. 1–2, pp. 23–42, 1992.

- [48] M. Baptistini and P. Táboas, “On the stability of some exponential polynomials,” *J. Math. Anal. Appl.*, vol. 205, no. 1, pp. 259–272, 1997.
- [49] R. Datko, “A procedure for determination of the exponential stability of certain differential-difference equations,” *Q. Appl. Math.*, vol. 36, no. 3, pp. 279–292, 1978.
- [50] Z. Wang, X. Li, and J. Lei, “Second moment boundedness of linear stochastic delay differential equations,” *Discrete Contin. Dyn. Syst. - B*, vol. 19, no. 9, pp. 2963 – 2991, 2014.
- [51] H. K. Khalil, *Nonlinear Systems*, ser. Pearson Education. Prentice Hall, 2002.
- [52] L. C. Westphal, *Root locus methods for analysis and design*. Boston, MA: Springer US, 2001, pp. 389–403.
- [53] D. R. Derryberry, *The Yule–Walker Equations and the Partial Autocorrelation Function*. John Wiley & Sons, Ltd, 2014, pp. 169–179.
- [54] E. I. Jury, “A simplified stability criterion for linear discrete systems,” *Proc. of the IRE*, vol. 50, no. 6, pp. 1493–1500, 1962.
- [55] L. Ballotta, M. R. Jovanović, and L. Schenato, “Optimal Network Topology of Multi-Agent Systems subject to Computation and Communication Latency (with proofs),” *arXiv:2101.10394*, Jan. 2021.
- [56] R. M. Gray, “Toeplitz and circulant matrices: A review,” *Foundations and Trends® in Communications and Information Theory*, vol. 2, no. 3, pp. 155–239, 2006.
- [57] C. Davis, “All convex invariant functions of Hermitian matrices,” *Archiv der Mathematik*, vol. 8, no. 4, pp. 276–278, 1957.
- [58] R. B. Nelson, “Simplified calculation of eigenvector derivatives,” *AIAA J.*, vol. 14, no. 9, pp. 1201–1205, 1976.
- [59] U. Prells and M. I. Friswell, “Calculating derivatives of repeated and nonrepeated eigenvalues without explicit use of eigenvectors,” *AIAA Journal*, vol. 38, no. 8, pp. 1426–1436, 2000.
- [60] M. I. Friswell, “The derivatives of repeated eigenvalues and their associated eigenvectors,” *J. Vib. Acoust.*, vol. 118, no. 3, pp. 390–397, July 1996.

APPENDIX

A. Proof of Proposition 2

The error dynamics equation with agent model (III.7) reads

$$dx(t) = (A_0x(t) + A_1x(t-1))dt + Bd\bar{w}(t), \quad (A.1)$$

$$A_0 = \begin{bmatrix} 0 & I \\ 0 & -\eta I \end{bmatrix}, \quad A_1 = \begin{bmatrix} 0 & 0 \\ -\eta K & 0 \end{bmatrix}, \quad B = \begin{bmatrix} 0 \\ I \end{bmatrix},$$

with $\bar{w}(t)$ standard N -dimensional Brownian motion. The decoupling (III.9) is obtained from (A.1) through the change of basis $x(t) = (T \otimes I_2)\tilde{x}(t)$. Rewriting (III.9) as a double integrator in state-space form with state $\tilde{s}_j(\cdot)$ yields

$$d\tilde{s}_j(t) = (F_0\tilde{s}_j(t) + F_{1j}\tilde{s}_j(t-1))dt + Gd\bar{w}_j(t), \quad (A.2)$$

$$F_0 = \begin{bmatrix} 0 & 1 \\ 0 & -\eta \end{bmatrix}, \quad F_{1j} = \begin{bmatrix} 0 & 0 \\ -\eta\lambda_j & 0 \end{bmatrix}, \quad G = \begin{bmatrix} 0 \\ 1 \end{bmatrix},$$

Stability of (A.1) is equivalent to that of (A.2) for all j . In the following, we drop the subscript j for the sake of readability. For positive eigenvalues λ , (A.2) is mean-square asymptotically stable if $\alpha_0 < 0$ and unstable if $\alpha_0 > 0$ [50], where the *spectral abscissa* is defined as

$$\alpha_0 \doteq \sup \{ \Re(z) : z \in \mathbb{C}, h(z) = 0 \}, \quad (A.3)$$

and the *characteristic polynomial* of (A.2) is

$$h(z) \doteq \det(zI - F_0 - F_1e^{-z}) = z^2 + \eta z + \eta\lambda e^{-z}. \quad (A.4)$$

A sufficient and necessary condition for all roots of $h(z)$ to lie in the open left-hand half-plane is derived in [48].

Theorem 1 ([48], Theorem 2.1). *Let the 2-vectors $v(b) = (pb, q - b^2)$, $w(b) = (\cos b, \sin b)$, $b \geq 0$, be given. If $r > 0$, a necessary and sufficient condition for all roots of the equation*

$h(z) = (z^2 + pz + q)e^z + r = 0$ to have negative real part is that the orthogonality condition $v(b) \cdot w(b) = 0$, with $b \in \cup_{k=0}^{\infty} (2k\pi, (2k+1)\pi)$, implies $|v(b)| > r$.

From Theorem 1, (A.2) is asymptotically stable if the following implication holds for $b \in \cup_{k=0}^{\infty} (2k\pi, (2k+1)\pi)$,

$$\eta b \cos b - b^2 \sin b = 0 \implies \eta^2 b^2 + b^4 > \eta^2 \lambda^2. \quad (A.5)$$

In view of $b \geq 0$ and $\sin b \geq 0$, (A.5) leads to (III.10) after standard algebraic manipulations, where we replace b with $\beta = \min b \in (0, \pi/2)$. The inequality can be rewritten as

$$\lambda < \frac{\beta}{\sin \beta} \doteq \phi(\eta), \quad (A.6)$$

where the definition of $\phi(\cdot)$ follows from the implicit function theorem applied to $F(\eta, \beta) \doteq \beta \tan \beta - \eta$, which states that $F(\eta, \beta) = 0$ if and only if $\beta = \varphi(\eta)$ and

$$\varphi'(\eta) = \frac{\cos^2(\varphi(\eta))}{\varphi(\eta) + \sin(\varphi(\eta)) \cos(\varphi(\eta))} \quad (A.7)$$

Tedious but straightforward calculations on the first and second derivatives show that $\phi(\eta)$ is concave increasing for any $\eta > 0$. The limits at 0 and $+\infty$ can be easily computed by noting that

$$\beta_0 \doteq \varphi(0) = 0, \quad \beta_{\infty} \doteq \lim_{\eta \rightarrow +\infty} \varphi(\eta) = \frac{\pi}{2}. \quad (A.8)$$

B. Derivation of First-Order Reduced Model for Continuous-Time Double Integrators

We now show that subsystem (III.9) can be approximated to first-order dynamics when the gain η is sufficiently high. Let us consider (A.2) with state $\tilde{s}(t) = [\tilde{x}(t), \tilde{z}(t)]^T$. Assume that the feedback gain η is large, so that the variable $\tilde{z}(t)$ evolves faster than $\tilde{x}(t)$. We can then approximate the dynamics of $\tilde{z}(t)$ by letting $\tilde{x}(t-1) \equiv x_0$ be constant overtime,

$$d\tilde{z}(t) = (-\eta\tilde{z}(t) - \eta\lambda x_0)dt + d\bar{w}(t). \quad (B.1)$$

Eq. (B.1) defines a standard Ornstein–Uhlenbeck process,

$$\tilde{z}(t) \sim \mathcal{N} \left(e^{-\eta t} (\tilde{z}(0) + \lambda x_0) - \lambda x_0, \frac{1}{2\eta} (1 - e^{-2\eta t}) \right). \quad (B.2)$$

In view of the time-scale separation, we assume that (B.2) holds (with $\tilde{x}(t-1)$ constant) till $\tilde{z}(t)$ settles at steady state,

$$\lim_{t \rightarrow +\infty} \tilde{z}(t) = \tilde{z}_{\infty} \sim \mathcal{N} \left(-\lambda x_0, \frac{1}{2\eta} \right). \quad (B.3)$$

Using (B.3), we now approximate the dynamics of $\tilde{x}(t)$ as if $\tilde{z}(t)$ reached the steady state instantaneously,

$$d\tilde{x}(t) \approx \tilde{z}_{\infty} dt = -\lambda \tilde{x}(t-1) dt + dn(t), \quad (B.4)$$

where the diffusion is embedded into the Brownian noise $n(t)$ with variance proportional to $1/\eta$. In particular, as $\eta \rightarrow +\infty$, $\tilde{z}_{\infty} \xrightarrow{a.s.} -\lambda x_0$ and (B.4) tends to deterministic dynamics.

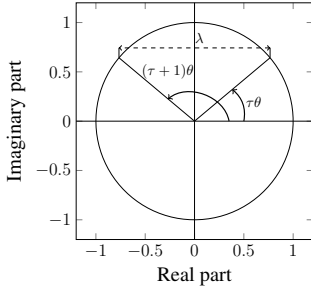


Fig. 8. A solution of (D.6) in the complex plane.

C. Computation of Suboptimal Variance for Continuous-Time Single Integrators

The N suboptimal eigenvalues have expression (cf. [56])

$$\tilde{\lambda}_j^* = 2\tilde{k}^* \left(n - \sum_{\ell=1}^n \cos \left(\frac{2\pi(j-1)\ell}{N} \right) \right), \quad (\text{C.1})$$

which we write as $\tilde{\lambda}_j^* = g_j(n)\tilde{k}^*$. Being $\tilde{k}^* = \tilde{\alpha}^*(n)\lambda^*$ according to Proposition 3, we write $\tilde{\lambda}_j^* = \tilde{c}_j^*(n)\lambda^*$ with $\tilde{c}_j^*(n) \doteq g_j(n)\tilde{\alpha}^*(n)$. Then, each subsystem (III.3) has variance

$$\begin{aligned} \sigma_I^2(\tilde{\lambda}_j^*) &= \frac{1 + \sin(\tilde{\lambda}_j^* \tau_n)}{2\tilde{\lambda}_j^* \cos(\tilde{\lambda}_j^* \tau_n)} \\ &\stackrel{(i)}{=} \frac{1 + \sin(\tilde{c}_j^*(n)\beta^*)}{2\tilde{c}_j^*(n)\beta^* \cos(\tilde{c}_j^*(n)\beta^*)} \tau_n = \tilde{C}_j^*(n)\tau_n, \end{aligned} \quad (\text{C.2})$$

where (III.6) is used in (i).

D. Stability Conditions for Discrete-Time Systems

General Case. In the following, we replace τ_n with τ for the sake of readability. For the single-integrator case, decoupling the error dynamics yields scalar subsystems of the form

$$\tilde{x}(k+1) = \tilde{x}(k) - \lambda\tilde{x}(k-\tau) + \tilde{w}(k). \quad (\text{D.1})$$

The characteristic polynomial $h(z)$ of (D.1) is obtained by applying the lag operator z such that $\tilde{x}(k)h(z) = \tilde{w}(k)$,

$$h(z) = z - 1 + \lambda z^{-\tau}. \quad (\text{D.2})$$

Similarly, the double-integrator decoupled subsystems are

$$\begin{aligned} \tilde{x}(k+1) &= \tilde{x}(k) + \tilde{z}(k) \\ \tilde{z}(k+1) &= (1-\eta)\tilde{z}(k) - \eta\lambda\tilde{x}(k-\tau) + \tilde{w}(k), \end{aligned} \quad (\text{D.3})$$

with characteristic polynomial

$$h(z) = z - 2 + \eta + (1-\eta)z^{-1} + \eta\lambda z^{-\tau-1}. \quad (\text{D.4})$$

For positive λ , stability of (D.1)–(D.3) can be assessed via the Jury stability criterion, which provides necessary and sufficient conditions for the roots of (D.2) and (D.4) to lie inside the unit circle in the form of inequalities involving the coefficients of $h(z)$. Being the latter polynomial in η and λ , the Jury criterion yields $\Theta(N\tau)$ polynomial inequalities in the feedback gains, which can be computed through standard software tools.

Proof of Proposition 4. Eq. (D.2) can be studied as a root locus by varying the gain λ . In particular, $\lambda = 0$ yields a

multiple root at $z_1^* = 0$ and a simple root at $z_2^* = 1$. Negative values of λ are discarded as they push the latter outside the unit circle. As λ increases, the branches leave the unit ball along their asymptotes. The admissible values for λ are upper bounded by a threshold gain λ_{th} beyond which some roots leave the unit ball. In particular, we are interested in the minimum gain for which at least one root lies exactly on the unit circle. Thus, we are looking for roots of (D.2) of the form $z = e^{j\theta}$,

$$e^{j(\tau+1)\theta} - e^{j\tau\theta} + \lambda = 0. \quad (\text{D.5})$$

Eq. (D.5) can be equivalently written as the system

$$\begin{cases} \cos((\tau+1)\theta) - \cos(\tau\theta) + \lambda = 0 \\ \sin((\tau+1)\theta) = \sin(\tau\theta). \end{cases} \quad (\text{D.6})$$

Fig. 8 depicts a solution of system (D.6) for $\sin(\tau\theta) > 0$. The case $\sin(\tau\theta) < 0$ is analogous and is omitted. Further, the solution $(\tau+1)\theta = \tau\theta$ can be discarded from the discussion, because it implies $\lambda = 0$ and thus prevents asymptotic stability. From elementary trigonometric arguments (c.f. Fig. 8), the second equation in (D.6) implies

$$\tau\theta + \frac{\theta}{2} = \frac{\pi}{2} + 2k\pi \rightarrow \theta = \frac{\pi + 4k\pi}{2\tau + 1}, \quad (\text{D.7})$$

where we impose $\theta \in [0, \pi]$ and thus $k \in \{0, \dots, \lfloor \tau/2 \rfloor\}$. This includes all possible cases, because the roots of (D.2) come in complex conjugates pairs. From (D.7), the first equation in (D.6), and the fact $\cos((\tau+1)\theta) = -\cos(\tau\theta)$, we retrieve

$$\lambda = 2 \cos \left(\frac{\pi\tau + 4k\pi\tau}{2\tau + 1} \right). \quad (\text{D.8})$$

The right-hand term in (D.8) is monotone increasing in k . Indeed, taking the argument of the cosine modulus 2π yields

$$\frac{\pi\tau + 4k\pi\tau}{2\tau + 1} \bmod 2\pi = \frac{\pi\tau - 2k\pi}{2\tau + 1} \in \left[0, \frac{\pi}{2}\right), \quad (\text{D.9})$$

which is nonnegative and monotone decreasing in k for any τ . Finally, the upper bound for the gain λ is given by

$$\lambda_{th} = \min_k 2 \cos \left(\frac{\pi\tau + 4k\pi\tau}{2\tau + 1} \right) = 2 \cos \left(\frac{\pi\tau}{2\tau + 1} \right). \quad (\text{D.10})$$

E. Variance Computation for Discrete-Time Systems

Wiener–Kintchine Formula. Given any fixed values of delay and feedback gains, the steady-state variance $\sigma_I^2(\lambda)$ or $\sigma_H^2(\eta, \lambda)$ of the decoupled subsystems can be computed numerically by

$$\frac{1}{2\pi} \int_{-\pi}^{+\pi} \frac{d\theta}{|h(e^{j\theta})|^2}, \quad (\text{E.1})$$

where the characteristic polynomial $h(z)$ is (D.2) or (D.4).

Single Integrator Model. The moment-matching method applied to the subsystem (D.1) yields a linear system of equations in the variables $(\rho_0, \dots, \rho_\tau)$, where $\rho_t \doteq \mathbb{E}[\tilde{x}(k)\tilde{x}(k \pm t)]$:

$$\rho_0 = \mathbb{E}[\tilde{x}(k+1)^2] = \rho_0 + \lambda^2 \rho_0 + 1 - 2\lambda \rho_\tau \quad (\text{E.2a})$$

$$\rho_1 = \mathbb{E}[\tilde{x}(k+1)\tilde{x}(k)] = \rho_0 - \lambda \rho_\tau \quad (\text{E.2b})$$

$$\vdots$$

$$\rho_\tau = \rho_{\tau-1} - \lambda \rho_1, \quad (\text{E.2c})$$

where (E.2b)–(E.2c) are the Yule-Walker equations. System (E.2) can be written compactly as $A^{(\tau)}\rho = e_1$, where $\rho^\top = [\rho_0, \dots, \rho_\tau]$, e_1 is the canonical vector in $\mathbb{R}^{\tau+1}$ with nonzero first coordinate and $A^{(\tau)} \in \mathbb{R}^{(\tau+1) \times (\tau+1)}$ with

$$A^{(\tau)} = \begin{bmatrix} -\lambda^2 & & & & 2\lambda \\ 1 & -1 & & & -\lambda \\ & \ddots & \ddots & \ddots & \\ & & -\lambda & 1 & -1 \end{bmatrix}. \quad (\text{E.3})$$

In particular, when τ is odd, the $(\lceil \tau/2 \rceil + 1)$ -th row is

$$[0 \ \dots \ 0 \ 1 \ -1 - \lambda \ 0 \ \dots \ 0], \quad (\text{E.4})$$

while, when τ is even, the $(\tau/2 + 2)$ -th row is

$$[0 \ \dots \ 0 \ 1 - \lambda \ -1 \ 0 \ \dots \ 0]. \quad (\text{E.5})$$

Notice that $A^{(\tau)}$ is full rank for all $\tau \geq 1$ and thus (E.2) can be solved uniquely. In particular, we are interested in the autocorrelation $\rho_0 = \sigma_f^2(\lambda)$, which is given by the ratio between the minor associated with the top-left element of $A^{(\tau)}$, named $n_\tau \doteq M_{1,1}^{(\tau)}$, and the determinant $d_\tau \doteq \det(A^{(\tau)})$. Specifically, ρ_0 is a rational function in λ and can be computed in closed form by a symbolic solver given any value of τ .

Further, n_τ and d_τ can be computed by leveraging the following nested structure of the matrix $A^{(\tau)}$:

$$A^{(\tau)} = \begin{bmatrix} -\lambda^2 & & & & -2\lambda \\ 1 & -1 & & & \\ & 1 & \boxed{\begin{matrix} -1 & & -\lambda \\ 1 & \boxed{\tilde{A}^{(\tau-4)}} & \\ -\lambda & 1 & -1 \end{matrix}} & & \\ & & -\lambda & 1 & -1 \\ -\lambda & & & & 1 \end{bmatrix}, \quad (\text{E.6})$$

where $\tilde{A}^{(\tau)}$ is the submatrix of $A^{(\tau)}$ obtained by removing its first row and column such that $M_{1,1}^{(\tau)} = \det(\tilde{A}^{(\tau)})$, and the matrices $\tilde{A}^{(\tau-2)}$ and $\tilde{A}^{(\tau-4)}$ are framed in (E.6).

The solution obeys the following recursive expression in τ :

$$n_\tau = \begin{cases} (-1 - \lambda)n_{\tau-1} + \tilde{n}_{\tau-1} & \text{if } \tau \text{ odd} \\ -(1 - \lambda)n_{\tau-1} - \lambda\tilde{n}_{\tau-1} & \text{if } \tau \text{ even,} \end{cases} \quad (\text{E.7a})$$

$$\tilde{n}_\tau = (2 - \lambda^2)\tilde{n}_{\tau-2} - \tilde{n}_{\tau-4}, \quad (\text{E.7b})$$

$$d_\tau = d_{\tau-2} - \lambda^2(n_\tau + n_{\tau-2}), \quad (\text{E.7c})$$

$$\tilde{n}_{-3} = -1 + \lambda^2, \ \tilde{n}_{-2} = \lambda^2, \ \tilde{n}_{-1} = -1, \ \tilde{n}_0 = 0, \quad (\text{E.7d})$$

$$n_{-1} = 0, \ n_0 = 1, \ d_{-1} = -2\lambda, \ d_0 = 2\lambda - \lambda^2. \quad (\text{E.7e})$$

Eq. (E.7) can be proved by an inductive argument on the delay τ .

Numerator. We demonstrate the formula for odd delays $\tau = 2k + 1, k \in \mathbb{N}$. The other case can be obtained similarly and is thus omitted.

Let us consider the submatrix $\tilde{A}^{(\tau)} \in \mathbb{R}^{\tau \times \tau}$ obtained by removing the first row and column of A , such that $n_\tau = \det(\tilde{A}^{(\tau)})$. Replacing the $(\lfloor \tau/2 \rfloor)$ -th column with the sum of $(\lfloor \tau/2 \rfloor)$ -th and $(\lceil \tau/2 \rceil)$ -th columns yields

$$\det(\tilde{A}^{(\tau)}) = \begin{vmatrix} \tilde{A}_{11}^{(\tau-1)} & & \tilde{A}_{12}^{(\tau-1)} \\ \dots & 0 & -\lambda & -1 - \lambda \\ & & 1 & \\ \tilde{A}_{21}^{(\tau-1)} & & 0 & \tilde{A}_{22}^{(\tau-1)} \\ & & \vdots & \end{vmatrix}, \quad (\text{E.8})$$

from which it follows $n_\tau = (-1 - \lambda)n_{\tau-1} - \det(R^{(\tau)})$ where $R^{(\tau)} \in \mathbb{R}^{(\tau-1) \times (\tau-1)}$ and the base case is $n_1 = -1 - \lambda$. This expression corresponds to (E.7a) with $\tilde{n}_{\tau-1} = -\det(R^{(\tau)})$. Manipulations of the second term yield a further recursive expression for $\tilde{n}_{\tau-1}$. Let us write

$$\det(R^{(\tau)}) = \begin{vmatrix} -1 & & & -\lambda \\ 1 & \boxed{\begin{matrix} -1 & & -\lambda \\ 1 & \boxed{R^{(\tau-4)}} & \\ \lambda & 1 & -1 \end{matrix}} \\ -\lambda & & 1 & -1 \end{vmatrix}, \quad (\text{E.9})$$

where the two inner boxes highlight $R^{(\tau-2)}$ and $R^{(\tau-4)}$, respectively. Straightforward calculations yield

$$\det(R^{(\tau)}) = \det(R^{(\tau-2)}) + \lambda \begin{vmatrix} 1 & \boxed{\begin{matrix} -1 & & -\lambda \\ 1 & \boxed{R^{(\tau-4)}} & \\ -\lambda & 1 & -1 \end{matrix}} \\ -\lambda & & 1 \end{vmatrix}. \quad (\text{E.10})$$

The determinant in the second addend is computed as

$$-\lambda \det(R^{(\tau-2)}) + \begin{vmatrix} 1 & \boxed{R^{(\tau-4)}} \\ -\lambda & 1 \end{vmatrix}, \quad (\text{E.11})$$

and the second addend in the above equation has the same structure as the determinant in the second addend in (E.10).

Thus, an easy inductive argument proves

$$\det(R^{(\tau)}) = \det(R^{(\tau-2)}) + \lambda \left(-\lambda \det(R^{(\tau-2)}) - \lambda \det(R^{(\tau-4)}) - \dots - \lambda \det(R^{(3)}) - \lambda \right), \quad (\text{E.12})$$

where the base case is $\det(R^{(3)}) = -\lambda^2$. Eq. (E.7b) is retrieved by noting

$$\det(R^{(\tau-2)}) - (1 - \lambda^2) \det(R^{(\tau-4)}) = \lambda \left(-\lambda \det(R^{(\tau-6)}) - \dots - \lambda \right), \quad (\text{E.13})$$

and thus the tail of the infinite summation in (E.12) can be replaced by the left-hand term in (E.13).

Denominator. The denominator of ρ_0 is computed as the determinant of A . Let $A^{(\tau)} \doteq A$, from (E.3) we get

$$\det(A^{(\tau)}) = -\lambda^2 M_{1,1}^{(\tau)} - 2\lambda \left| \begin{array}{cc|cc|cc|cc} 1 & -1 & & & & & & \\ & 1 & -1 & & & & & \\ & & 1 & -\lambda & & & & \\ & & & 1 & \tilde{A}^{(\tau-4)} & & & \\ & & & & & 1 & -1 & \\ -\lambda & & & & & & 1 & \end{array} \right|, \quad (\text{E.14})$$

where $\tilde{A}^{(\tau-2)}$ and $\tilde{A}^{(\tau-4)}$ are framed in the second addend above. The latter can be computed as the following sum,

$$\lambda M_{1,1}^{(\tau-2)} + \left| \begin{array}{cc|cc|cc} 1 & -1 & & & & \\ & 1 & & & & \\ & & \tilde{A}^{(\tau-4)} & & & \\ & & & 1 & & \\ -\lambda & & & & 1 & \end{array} \right|, \quad (\text{E.15})$$

where the same structure is repeated recursively in the second addend above. Thus, an easy inductive argument proves

$$d_\tau = -\lambda^2 n_\tau - 2\lambda (\lambda n_{\tau-2} + \lambda n_{\tau-4} + \dots + \lambda n_1 + 1), \quad (\text{E.16})$$

where the base case is $d_1 = -\lambda^2(-1 - \lambda) - 2\lambda$. Eq. (E.7c) is retrieved by noting

$$\begin{aligned} -2\lambda (\lambda n_{\tau-2} + \lambda n_{\tau-4} + \dots + 1) &= \\ -\lambda^2 n_{\tau-2} - \lambda^2 n_{\tau-4} - 2\lambda (\lambda n_{\tau-4} + \dots + 1) &= \\ -\lambda^2 n_{\tau-2} + d_{\tau-2}. \end{aligned} \quad (\text{E.17})$$

Given τ , convexity of ρ_0 in λ can be assessed by checking the sign of the second derivative in the stability region. This reduces to a system of inequalities which can be solved, *e.g.*, by `solve_rational_inequalities` in Python. The variance was proved strictly convex for all tried delays.

Double Integrator Model. The moment-matching system associated with (D.3) has $\tau + 2$ variables $(\rho_0, \dots, \rho_{\tau+1})$ and

is composed of the following equations:

$$\begin{aligned} \rho_0 &= (2 - \eta)^2 \rho_0 + (1 - \eta)^2 \rho_0 + \eta^2 \lambda^2 \rho_0 + 1 \\ &\quad - 2(2 - \eta)(1 - \eta) \rho_1 - 2(2 - \eta) \eta \lambda \rho_{\tau+1} \\ &\quad + 2(1 - \eta) \eta \lambda \rho_\tau \end{aligned} \quad (\text{E.18a})$$

$$\rho_1 = (2 - \eta) \rho_0 - (1 - \eta) \rho_1 - \eta \lambda \rho_{\tau+1} \quad (\text{E.18b})$$

$$\rho_2 = (2 - \eta) \rho_1 - (1 - \eta) \rho_0 - \eta \lambda \rho_\tau \quad (\text{E.18c})$$

$$\vdots$$

$$\rho_{\tau+1} = (2 - \eta) \rho_\tau - (1 - \eta) \rho_{\tau-1} - \eta \lambda \rho_1, \quad (\text{E.18d})$$

where (E.18b)–(E.18d) are the Yule-Walker equations associated with (D.3). Analogous considerations to the single-integrator model can be done in this case.